Appl. Phys. A
DOI 10.1007/s00339-014-8245-2

Applied Physics A
Materials Science & Processing

Impact of amorphization on the magnetic state and magnetocaloric properties of Gd_3Ni

D. A. Shishkin · N. V. Baranov · A. F. Gubkin · A. S. Volegov · E. G. Gerasimov · P. B. Terentev · L. A. Stashkova

Received: 1 November 2013 / Accepted: 8 January 2014

Abstract Rapid quenching and ball milling have been used to modify the magnetic state and magnetocaloric properties of the intermetallic compound Gd_3Ni. The melt-spun and ball-milled Gd_3Ni samples are found to exhibit a soft ferromagnetic-like behavior below 120 K, whereas in the crystalline state, the Gd_3Ni compound is an antiferromagnet with a Néel temperature of about 99 K. The reduced value of the saturation magnetization observed in amorphous Gd_3Ni samples is ascribed to the appearance of a magnetic moment on Ni atoms. After amorphization, the Gd_3Ni samples exhibit substantially improved magnetocaloric properties in a low field region in comparison with crystalline Gd_3Ni.

1 Introduction

Currently, there is an increased interest in materials with enhanced magnetocaloric effect (MCE). This is due to the possibility of using these materials to create cooling devices operating in different temperature ranges [1–4]. The magnetocaloric effect is characterized by an adiabatic temperature change (ΔT_{ad}) and isothermal magnetic entropy change (ΔS_M) with varying magnetic fields [2, 5]. The maximal ΔS_M and ΔT_{ad} values are observed in the vicinity of the magnetic phase transitions where the magnetization of a material changes rapidly with temperature. The largest MCE is detected in materials undergoing a first-order magnetic phase transition [6, 7]. However, the high MCE in such materials is reached as a rule within a narrow temperature range; moreover, the first-order phase transitions can be accompanied by hysteresis which decreases the efficiency of magnetic refrigeration. Among compounds exhibiting a second-order magnetic phase transition, most attention has been paid to compounds based on rare-earth metals (R) including rare-earth-containing amorphous alloys. This is because other properties such as electrical resistivity and corrosion resistance as well as mechanical properties are important from the practical point of view. The rapid quenching from the melt allows preparing amorphous alloys with various contents of components and magnetic ordering temperatures and, therefore, to obtain materials with high MCE realized within different temperature ranges.

The aim of the present work is to study the influence of amorphization by using different techniques on the magnetic state and magnetothermal properties of Gd_3Ni. The preliminary results of this work have already been reported [8]. The intermetallic compound Gd_3Ni having the highest Gd concentration within the Gd–Ni family crystallizes in a low-symmetry orthorhombic Fe_3C-type structure (the Pnma space group) [9] and shows an antiferromagnetic (AF) behavior below the Néel temperature $T_N \sim$ (96–101.5) K [10–14]. The magnetization measurements on a single crystal of Gd_3Ni [12] have revealed that the first-order magnetic phase transition takes place at a critical magnetic field, H_c, of about 40 kOe when the magnetic field is applied along the *b*- or *c*-axes, while along the *a*-axis, the magnetization shows a gradual growth with increasing field up to the saturation. The magnetic structure of Gd_3Ni has not been

D. A. Shishkin · N. V. Baranov · A. F. Gubkin · E. G. Gerasimov · P. B. Terentev · L. A. Stashkova
Institute of Metal Physics, Russian Academy of Science, 620990 Ekaterinburg, Russia

D. A. Shishkin (✉) · N. V. Baranov · A. F. Gubkin · A. S. Volegov
Institute of Natural Sciences, Ural Federal University, 620083 Ekaterinburg, Russia
e-mail: shishkin@imp.uran.ru

Published online: 22 January 2014

determined yet, since Gd has a high neutron absorption cross section. As was suggested from single-crystal magnetization data, the Gd-magnetic moments in Gd_3Ni lie predominantly parallel to the *bc* plane of the orthorhombic unit cell [12]. There are no evidences that Ni atoms have an ordered magnetic moment in this compound. From the magnetization data for polycrystalline Gd_3Ni, the ΔS_M value was reported to be equal to −5 J/kg K at a magnetic field change from 0 to 5 T in the vicinity of the Néel temperature [15]. The magnetic properties of amorphous Gd–Ni alloys were studied mainly for the Gd concentrations close to 67 at.% [16–18]. To our knowledge there are no published data on the magnetic state and magnetothermal properties of amorphous Gd–Ni alloy containing 75 at.% Gd. Another goal of this work is to achieve a better understanding of the formation of magnetic moments on 3*d*-metal atoms in amorphous rare earth–transition metal alloys.

2 Experimental details

Polycrystalline samples of Gd_3Ni were synthesized by arc melting of the constituent elements in a high-purity argon atmosphere. For the crystalline samples, we used gadolinium metal of 99.8 % purity and electrolytic nickel (99.99 %) which was pre-annealed under vacuum. To compensate for the evaporation of gadolinium during the melting process in an arc furnace, an excess of gadolinium of 0.4 wt% was used. The ingots were remelted several times to achieve a good homogeneity of the samples. Amorphous Gd_3Ni ($Gd_{75}Ni_{25}$) alloys were prepared by a melt-spinning technique in argon atmosphere onto a rotating copper wheel with a tangential speed up to 50 m/s and also by ball milling in an evacuated brass mortar for 20 h. After ball milling, the Gd_3Ni powder was stored in an evacuated ampoule to prevent oxidation until magnetic measurements. The structure of the samples was examined using a DRON-type X-ray diffractometer with monochromatic Cr Kα radiation. The magnetic measurements were carried out using a SQUID magnetometer (MPMS, Quantum Design, USA) in magnetic fields up to 70 kOe in the temperature range from 2 up to 600 K. The high-field magnetization measurements were carried out at 4.2 K in a pulsed magnetic field up to 350 kOe by an induction method using a wire-wound pulsed magnet with a duration time of about 10 ms.

3 Results and discussion

The X-ray diffraction (XRD) patterns for the samples obtained by liquid quenching (LQ) and ball milling (BM) are presented in Fig. 1. The pattern for the polycrystalline Gd_3Ni sample is shown as well for the comparison. As one can see, the patterns for liquid-quenched ribbons and ball-milled alloys exhibit a broad peak in the range of $40° < 2\Theta < 55°$ indicating that the samples are mostly amorphous. The presence of some Bragg peaks on the XRD pattern for the LQ (35 m/s) sample obtained at a linear speed of 35 m/s indicates that this sample contains an amorphous matrix with a small amount of crystalline phase of Gd_3Ni and Gd_2O_3 oxide. Some traces of the Gd_2O_3 oxide were also detected in other amorphous samples.

Figure 2 displays the temperature dependences of the magnetic susceptibility of Gd_3Ni samples in crystalline and amorphous states. The maximum on the $\chi(T)$ curve at $T = 99$ K for the crystalline Gd_3Ni corresponds to the Néel temperature, which is in agreement with previously reported data [10–14]. After amorphization, the magnetic state of Gd_3Ni is observed to be substantially modified. As follows from the susceptibility data, both LQ (50 m/s) and BM samples demonstrate a ferromagnetic-like behavior with Curie temperatures 118 and 123 K, respectively. We did not observe any anomalies around 294 K, which could be associated with magnetic phase transition in pure Gd. The $\chi(T)$ curves for amorphous LQ (35 m/s) and BM samples obey the Curie–Weiss law above 200 K (shown in the insets in Fig. 2a, b). The value of the paramagnetic Curie temperature, Θ_p, is obtained to be 158 and 138 K for the LQ (35 m/s) and BM samples, respectively, and $\Theta_p = 57.9$ K [12] for the crystalline counterpart. The increased Θ_p values are indicative of the enhancement of positive exchange interactions in Gd_3Ni after amorphization. The effective magnetic moment, μ_{eff}, per Gd atom is estimated to be 8.09 and 8.47 μ_B for LQ (35 m/s) and BM

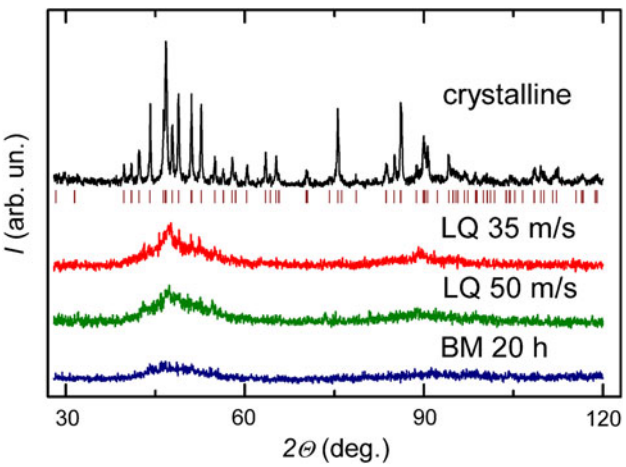

Fig. 1 X-ray diffraction patterns of the crystalline, liquid-quenched (LQ) and ball-milled (BM) samples of Gd_3Ni. The *vertical bars* indicate the calculated Bragg peaks positions for an orthorhombic structure described by the *Pnma* space group

Gd_3Ni samples, respectively. These values are slightly higher than $\mu_{eff} = 7.94\ \mu_B$ for the Gd^{3+} free ion. The crystalline Gd_3Ni was observed to exhibit an enhanced μ_{eff} value as well [11]. The susceptibility of the LQ (50 m/s) sample (see inset in Fig. 2a) does not follow the Curie–Weiss law up to ~270 K, which can be associated with the persistence of short-range magnetic order in the paramagnetic state. The deviation of the susceptibility from the Curie–Weiss law over a wide temperature range above T_C was also detected for the amorphous $Gd_{67}Ni_{33}$ ferromagnet, which was ascribed to the presence of short-range magnetic correlations [16]. The persistence of short-range correlations up to temperatures greater than 5–6 times the Néel temperature was observed recently in some crystalline R_3Ni and R_3Co compounds with R = Gd and Tb [19].

As follows from Fig. 3, the magnetization process in Gd_3Ni is changed dramatically after amorphization. Unlike the polycrystalline Gd_3Ni sample which shows a spin-flop-like phase transition, the amorphous sample demonstrates a soft ferromagnetic behavior. For the LQ (35 m/s) sample, a small anomaly on the magnetization curve around 40 kOe is observed, which can be associated with the presence of the residual crystalline Gd_3Ni phase. However, we did not observe any anomalies on the magnetization curves for amorphous Gd_3Ni alloys prepared by melt spinning with the wheel speed of 50 m/s as well as by ball milling. The measurements in high-pulsed magnetic fields (shown in Fig. 4) have revealed that the magnetization of both amorphous and crystalline samples saturates at $H > 100$ kOe. The saturation magnetic moments per formula unit (μ_{FU}) reaches 23.3 μ_B and 19.8 μ_B for crystalline and amorphous LQ (50 m/s) samples, respectively. Suggesting that the nickel atoms do not carry magnetic moment in the crystalline Gd_3Ni, we obtain the saturation magnetic moment per Gd atom $\mu_S(Gd) = 7.77\ \mu_B$. This value is slightly higher than that obtained for pure Gd metal (7.63 μ_B [20]) and together with 7 μ_B from the half-filled 4*f* shell presumably includes an induced conduction electron moment. Bearing in mind that the exchange interaction between 4*f* and 3*d* spins in all rare earth transition metal compounds is antiferromagnetic [21], a lower value of the saturation magnetic moment in the amorphous Gd_3Ni may be ascribed to the presence of an induced moment of about 1.2 μ_B on Ni atoms. It is worth mentioning that the exchange interactions in rare earth–transition metal compounds are rather complex (see [21], for instance). According to the Campbell's model [22] which is accepted at present in literature, the 4*f* electrons of the rare earth polarize their 5*d* bands and there are short-range 5*d*–3*d* exchange interactions with neighboring 3*d* atoms. The 4*f* and 5*d* moments are aligned parallel since the local 4*f*–5*d* exchange interaction is positive, while the short-range exchange and hybridization effects between the 5*d* and 3*d* electrons result in the antiparallel alignment of the 4*f* and 3*d* spins. However, the total 4*f* magnetic moment which includes spin and orbital contributions is coupled with 3*d*-metal moment ferromagnetically in the case of light rare earths and antiferromagnetically in compounds with heavy rare-earth metals [21]. In crystalline Gd–Ni compounds with high Gd concentrations, fairly low magnetic moments (μ_{Ni}) are observed on Ni atoms, and a value of μ_{Ni} decreases with the Gd concentrations (~0.2 μ_B for $GdNi_2$ [23] and ~0.1 μ_B for GdNi [24]). However, according to the magnetic Compton profile measurements [25], the Ni atoms exhibit a substantially increased moment in the amorphous $Gd_{50}Ni_{50}$ alloy ($\mu_{Ni} \approx 0.55\ \mu_B$). Moreover, from analysis of the spontaneous volume magnetostriction, the Ni moment of 0.61 μ_B per atom was suggested to exist in a melt-spun amorphous alloy $Gd_{67}Ni_{33}$ with higher Gd concentration

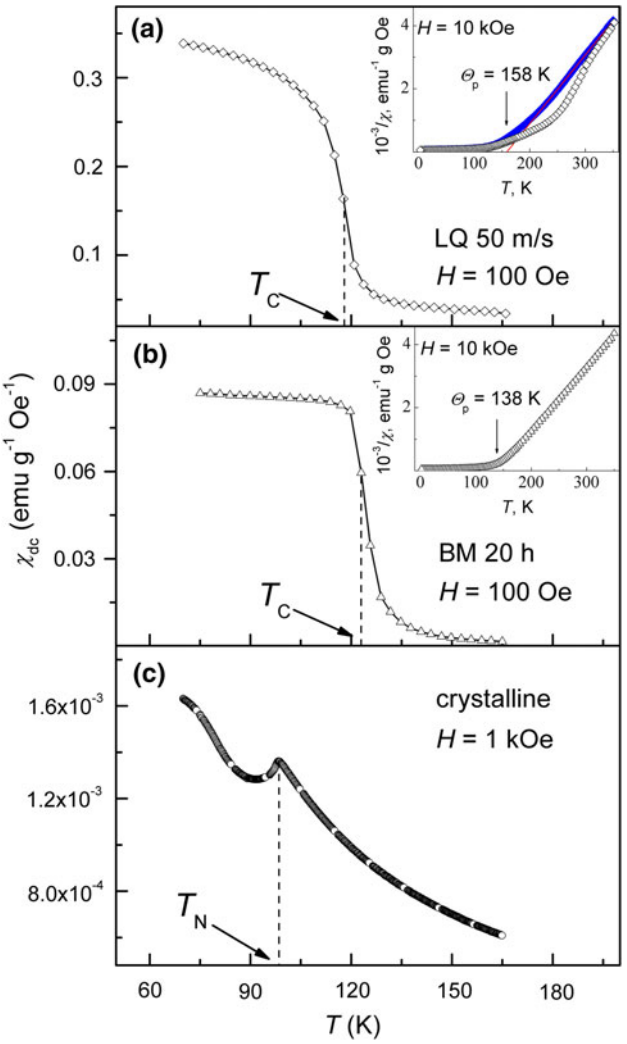

Fig. 2 Temperature dependences of the DC susceptibility for amorphous (*a*, *b*) and crystalline (*c*) Gd_3Ni alloys. The *insets* show the reciprocal DC susceptibility versus temperature measured at $H = 10$ kOe for LQ (35 m/s—*full symbols*; 50 m/s—*open symbols*) and BM (*open triangles*) alloys

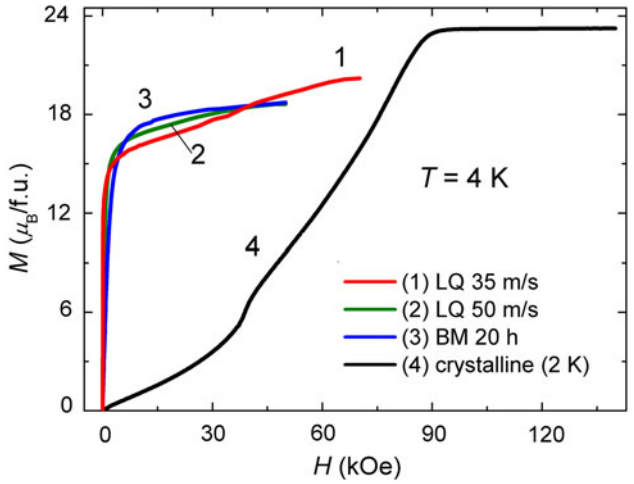

Fig. 3 Magnetization curves for the amorphous Gd_3Ni alloys at $T = 4$ K in comparison with $M(H)$ dependences for their polycrystalline counterpart at $T = 2$ K. The magnetization curve for the crystalline Gd_3Ni compound is taken from [19]

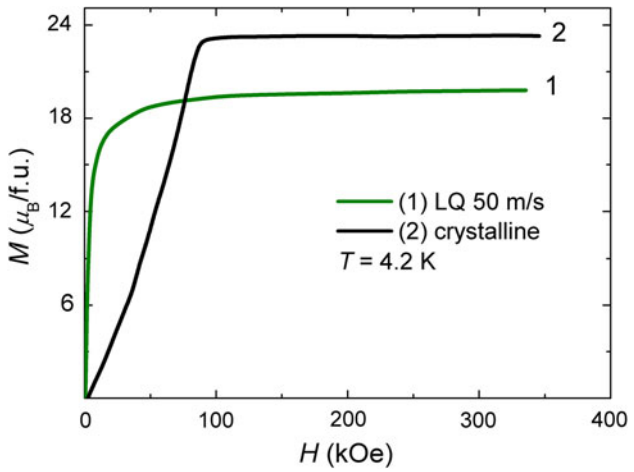

Fig. 4 Magnetization isotherms of the amorphous LQ (50 m/s) and polycrystalline Gd_3Ni samples in high-pulsed magnetic fields at $T = 4.2$ K

[26]. The μ_{Ni} value $\sim 1.2\ \mu_B$ derived from our high-field magnetization data for the amorphous Gd_3Ni seems to be unexpectedly high. Further examination is required to find out whether amorphization is responsible for such a difference in the magnetic state of Ni atoms in crystalline and amorphous states.

As for the magnetothermal properties of Gd_3Ni, the isothermal magnetic entropy change ΔS_M can be calculated by integrating the Maxwell relationship [2]:

$$\Delta S_M(T, \Delta H) = \int_0^{H_{max}} \left(\frac{\partial M}{\partial T}\right)_H dH \quad (1)$$

where H_{max} is the final applied magnetic field. The temperature dependences of ΔS_M, presented in Fig. 5,

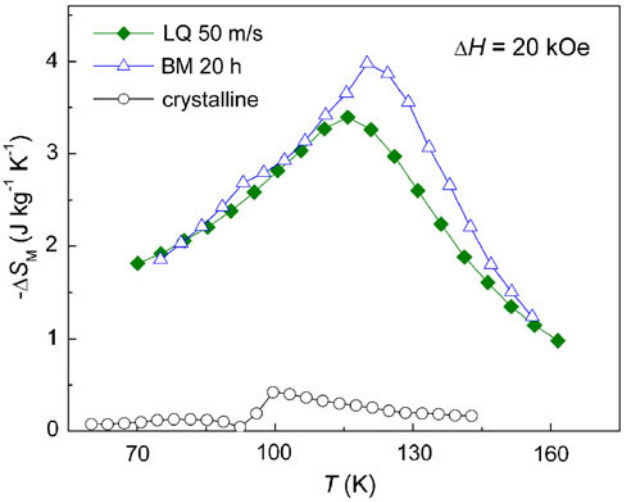

Fig. 5 Temperature dependences of the magnetic entropy change for the amorphous Gd_3Ni alloys in comparison with their polycrystalline counterpart at a magnetic field change ΔH of 20 kOe

were calculated using Eq. (1) from a typical set of selected $M(T)$ curves measured at various magnetic fields. Taking into account the amorphization-induced changes in the magnetic state and, consequently, in the shape of the $M(T)$ curves, the enhancement of magnetocaloric properties at low fields could be expected for amorphous alloys. The maximum values of $|\Delta S_M|$ at $\Delta H = 20$ kOe were found to be 3.4 J/kg/K for LQ (50 m/s) and 4.0 J/kg/K for BM alloys which exceed more than eight times the ΔS_M value for the crystalline Gd_3Ni compound at the same field change. The relative cooling power (RCP) which indicates how much heat can be transferred between the cold and hot sinks of a refrigerator in one ideal thermodynamic cycle was estimated as [1]:

$$RCP(S) = -\Delta S_M(\max) \times \delta T_{FWHM} \quad (2)$$

where δT_{FWHM} is the full width at half maximum of ΔS_M peak. The RCP values for both LQ (50 m/s) and BM samples were estimated to be 273 and 259 J/kg, respectively. These values were found to be 20 times higher than that for their crystalline counterpart.

4 Conclusions

The comparative study of the magnetic and magnetocaloric properties of amorphous Gd_3Ni alloys and their crystalline counterpart reveals that amorphization leads to the cardinal change in the magnetic state of the material. Unlike an antiferromagnetic order observed in the crystalline Gd_3Ni compound, the amorphous samples with the same composition demonstrate a soft ferromagnetic-like behavior. Moreover, amorphous Gd_3Ni alloys exhibit a higher

magnetic ordering temperature which indicates an increase in the exchange interaction energy. The reduced value of the saturation magnetization observed in Gd_3Ni after amorphization may result from the appearance of a magnetic moment on Ni atoms and antiparallel alignment of 4*f* and 3*d* moments. Thus, the magnetic order of the amorphous Gd_3Ni alloy can be rather characterized as a ferrimagnetic one. The impact of amorphization manifests itself most substantially in the increase of the isothermal magnetic entropy change (more 8 times) and relative cooling power (about 20 times) upon application of the external magnetic field of 20 kOe. The results of the present work show that the antiferromagnetic compounds being amorphized may considered for application to magnetic refrigeration.

Acknowledgments The authors are grateful to Dr. M. Uimin (Institute of Metal Physics, Ekaterinburg, Russia) for the amorphization of Gd_3Ni by ball milling. This work was supported in part by the program of the Presidium RAS (Project No. 12-P-23-2005), by the Russian Foundation for Basic Research (Grants No. 10-02-96028 and No. 14-02-31865) and the Ministry of Education and Science of the Russian Federation (Contract No. 14.518.11.7020).

References

1. K.A. Gschneidner Jr., V.K. Pecharsky, in *Intermetallic Compounds: Principles and Practice. V. 3: Progress*, ed. by J.H. Westbrook, R.L. Fleischer (Wiley, Chichester, 2002), p. 519
2. K.A. Gschneidner Jr, V.K. Pecharsky, A.O. Tsokol, Rep. Prog. Phys. **68**, 1479 (2005)
3. E. Brück, O. Tegus, D.T.C. Thanh, K.H.J. Buschow, J. Magn. Magn. Mater. **310**, 2793 (2007)
4. K.A. Gschneidner Jr, V.K. Pecharsky, Int. J. Refrig. **31**, 945 (2008)
5. N.A. de Oliveira, P.J. von Ranke, Phys. Rep. **489**, 89 (2010)
6. M. Khan, S. Stadler, N. Ali, J. Appl. Phys. **101**, 09C515 (2007)
7. B.R. Gautam, I. Dubenko, J.C. Mabon, S. Stadler, N. Ali, J. Alloys Compd. **472**, 35 (2009)
8. D.A. Shishkin, N.V. Baranov, A.V. Proshkin, S.V. Andreev, A.S. Volegov, Solid State Phenom. **190**, 355 (2012)
9. D.T. Cromer, A.C. Larson, Acta Cryst. **14**, 1226 (1961)
10. G.J. Primavesi, K.N.R. Taylor, J. Phys. F: Metal. Phys. **2**, 761 (1972)
11. E. Talik, Phys. B **193**, 213 (1994)
12. N.V. Tristan, S.A. Nikitin, T. Palewski, K. Skokov, J. Warchulska, J. Alloys Compd. **334**, 40 (2002)
13. N.V. Tristan, K. Nenkov, K. Skokov, T. Palewski, Phys. B **344**, 462 (2004)
14. N.V. Baranov, H. Michor, G. Hilscher, A. Proshkin, A. Podlesnyak, J. Phys. Condens. Matter **20**, 325233 (2008)
15. S.K. Tripathy, K.G. Suresh, A.K. Nigam, J. Magn. Magn. Mater. **306**, 24 (2006)
16. I. Nakai, T. Fukagawa, J. Phys. Soc. Jpn. **62**, 2456 (1993)
17. K.H.J. Buschow, J. Magn. Magn. Mater. **21**, 97 (1980)
18. X.C. Zhong, P.F. Tang, Z.W. Liu, D.C. Zeng, Z.G. Zheng, H.Y. Yu, W.Q. Qiu, M. Zou, J. Alloys Compd. **509**, 6889 (2011)
19. N.V. Baranov, A.V. Proshkin, A.F. Gubkin, A. Cervellino, H. Michor, G. Hilscher, E.G. Gerasimov, G. Ehlers, M. Frontzek, A. Podlesnyak, J. Magn. Magn. Mater. **324**, 1907 (2012)
20. L.W. Roeland, G.J. Cock, F.A. Muller, A.C. Moleman, K.A. McEwen, R.G. Jordan, D.W. Jones, J. Phys. F: Met. Phys. **5**, L233 (1975)
21. N.H. Duc, in *Handbook on the Physics and Chemistry of Rare Earths*, Vol. 24, ed. by K.A. Gschneidner Jr., L. Eyring (Elsevier Science B.V., 1997), p. 339
22. I.A. Campbell, J. Phys. F: Met. Phys. **2**, L47 (1972)
23. M. Mizumaki, K. Yano, I. Umehara, F. Ishikawa, K. Sato, A. Koizumi, N. Sakai, T. Muro, J. Phys. Rev. B **67**, 132404 (2003)
24. K. Yano, I. Umehara, K. Sato, A. Yaresko, J. Solid State Commun. **136**, 67 (2005)
25. T. Kurachi, K. Yano, H. Sakurai, M. Ota, H. Adachi, H. Kawata, Foton factory activity report 2006 #24, 92 (2007)
26. I. Nakai, H. Tange, K. Konishi, T. Kamimori, A. Chikazawa, Y. Motegi, J. Phys. Soc. Jpn. **72**, 1184 (2003)